AIP | Applied Physics Letters

All-chalcogenide glass omnidirectional photonic band gap variable infrared filters

H. Esat Kondakci, Mecit Yaman, Ozlem Koylu, Aykutlu Dana, and Mehmet Bayindir

Citation: Appl. Phys. Lett. **94**, 111110 (2009); doi: 10.1063/1.3103279
View online: http://dx.doi.org/10.1063/1.3103279
View Table of Contents: http://apl.aip.org/resource/1/APPLAB/v94/i11
Published by the American Institute of Physics.

All-chalcogenide glass omnidirectional photonic band gap variable infrared filters

H. Esat Kondakci,[1,2,a)] Mecit Yaman,[1] Ozlem Koylu,[1] Aykutlu Dana,[1] and Mehmet Bayindir[1,2,b)]
[1]*UNAM-Institute of Materials Science and Nanotechnology, Bilkent University, 06800 Ankara, Turkey*
[2]*Department of Physics, Bilkent University, 06800 Ankara, Turkey*

(Received 10 January 2009; accepted 26 February 2009; published online 18 March 2009)

We report on the design, fabrication, and characterization of spatially variable infrared photonic band gap filter that consists of thermally evaporated, high refractive index contrast, amorphous chalcogenide glass multilayers. Due to graded thickness structure, the filter exhibits a position dependent stop band and a cavity mode ranging from 1.8 to 3.4 μm wavelengths. Reflection measurements on the variable filter agree well with theoretical calculations. These results pave the way to low-loss infrared mirrors, filters, spectral imaging, and miniaturized spectrometers at infrared region. © *2009 American Institute of Physics*. [DOI: 10.1063/1.3103279]

Dielectric mirrors are simple one-dimensional photonic structures made using quarter wave stacks (QWSs).[1] It was recently shown that QWS fabricated with high contrast index materials may posses full photonic band gaps resulting in omnidirectional reflection,[2,3] which opens up the possibility of making infrared (IR) mirrors[4] and filters[5–7] at specific wavelengths by choosing suitable dielectric materials and by controlling layer thicknesses. Such optical components are critical in designing spectrometers, military applications, and chemical and biological sensors at the IR region.[8]

The QWS structures can be obtained by chemical vapor deposition,[9] sol-gel processing,[10] molecular beam epitaxy,[11] spin coating/thermal evaporation,[3] or thermal evaporation.[12] In addition to the above-mentioned techniques the amorphous chalcogenide glasses can be thermally evaporated on the large area polymer films.[13] In this case the radial QWSs are obtained by rolling the coated polymer film on a cylindirical rod. Subsequently, the macroscopic structures are drawn into various photonic band gap fibers at visible[5,6] and IR wavelengths.[4] Although the radial polymer/chalcogenide multilayers form otherwise a perfect omnidirectional mirror, which guides light through the hollow core of the transmission fibers, the strong absorption of polymer layers at IR region limits reducing the transmission loss further.

Since chalcogenide glasses have unique properties such as high refractive indices and transparency at IR region, they are excellent materials to be used in omnidirectional photonic applications.[6,14,15] For example, by using all-chalcogenide photonic band gap structures one can reduce the transmission losses in hollow-core fibers. Moreover, omnidirectional mirrors and filters can be used in order to design miniaturized IR spectrometers.

In this work, we present an omnidirectional QWS consisting of high refractive index contrast chalcogenide glasses that are thermally evaporated on a substrate consecutively. A spatially variable IR Fabry–Pérot filter is designed and fabricated by thermal evaporation on a tilted silicon substrate, as shown in Figs. 1(a) and 1(b). The filter consists of alternating low-index As_2S_3 and high-index $Ge_{15}As_{25}Se_{15}Te_{45}$ (GAST) stacks with an As_2S_3 cavity layer [Fig. 1(c)]. The utilization of high-index contrast chalcogenide glasses in a slanted geometry results in a position dependent full photonic band gap and cavity mode. The structures are simulated by using the generalized transfer matrix method for coherent and incoherent multilayer structures with finite substrates.[16] We observed that the cavity wavelength shifts from 1.8 to 3.4 μm on a 5 cm long substrate.

The high-index chalcogenide GAST glass was synthesized from high-purity (5–6*N*) Ge, As, Se, and Te elements (Alfa Aesar) using conventional sealed-ampoule melt-quenching techniques.[17,18] For the low-index material, As_2S_3 (Amorphous Materials) was chosen due to thermal compatibility with GAST glass. To characterize optical properties of As_2S_3 and GAST thin films, bulk glasses were deposited on

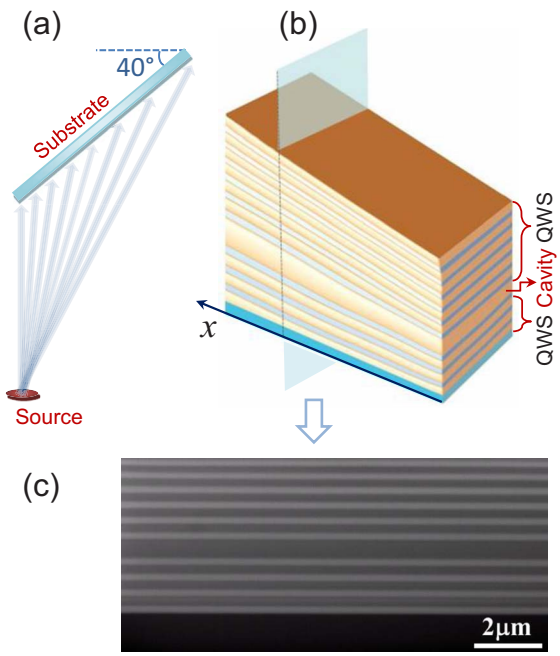

FIG. 1. (Color online) Schematic representation of (a) slanted evaporation geometry and (b) spatially variable multilayer filter structure. (c) Cross-sectional scanning electron micrograph of the 20 layer As_2S_3–$Ge_{15}As_{25}Se_{15}Te_{45}$ multilayer structure. The dark layers correspond to As_2S_3 layers with a $\lambda/2n$ cavity layer.

a)Electronic mail: kondakci@bilkent.edu.tr.
b)Electronic mail: bayindir@nano.org.tr. URL: http://bg.bilkent.edu.tr.

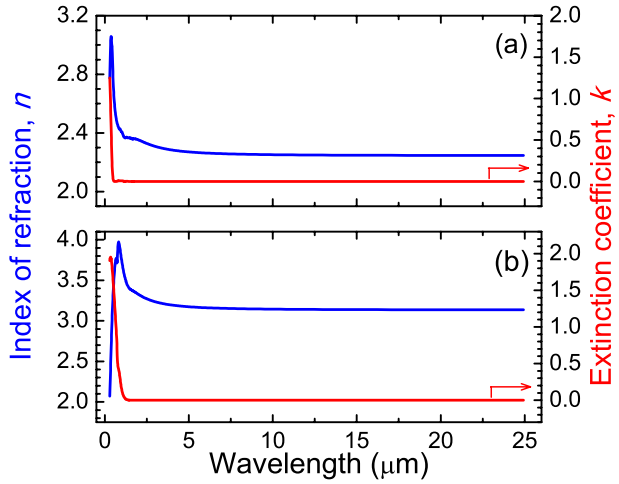

FIG. 2. (Color online) Measured index of refraction and extinction coefficient of (a) thermally evaporated As_2S_3 and (b) $Ge_{15}As_{25}Se_{15}Te_{45}$ thin films. The refractive index contrast allows to achieve omnidirectional photonic band gap.

silicon substrates by thermal evaporation (Vaksis Elif, pressure of $\sim 10^{-6}$ Torr, deposition rate of ~ 100 Å/s). Subsequently, the films were annealed for 2 h near the glass transition temperature 190 °C in a vacuum oven.

The refractive index n and the extinction coefficient k of the deposited films are obtained in the visible and mid-IR region from spectroscopic ellipsometry measurements (J. A. Woollam VASE, IR-VASE).[19] As shown in Fig. 2, both chalcogenide glasses are transparent between 1.5 and 25 μm. At 3 μm, GAST and As_2S_3 has a high-index ratio of 3.22:2.33, which is required for achieving an omnidirectional photonic band gap.

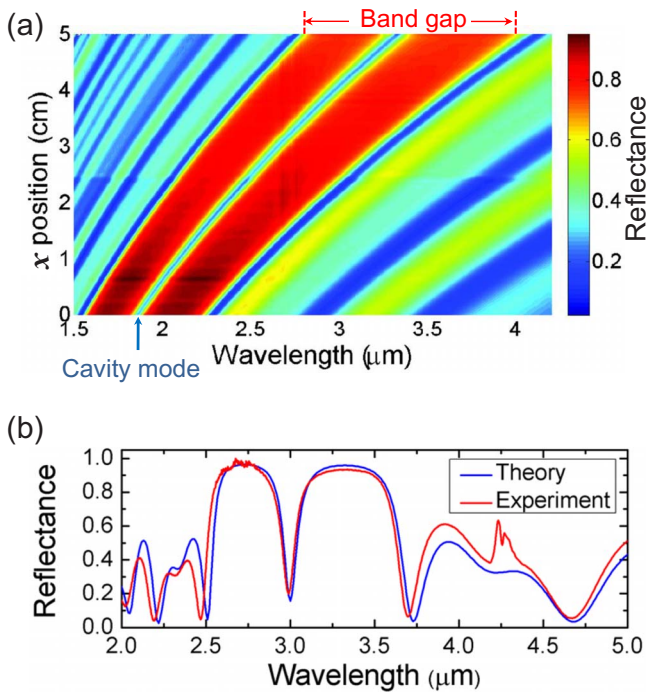

FIG. 3. (Color online) (a) Position dependent reflectance measurements taken from 80 linearly spaced positions along the sample. (b) Comparison of theoretical and experimental reflectance spectra taken at a position 4 cm away from the short-wavelength side of the filter. Both the simulation and FTIR measurements are performed at normal incidence.

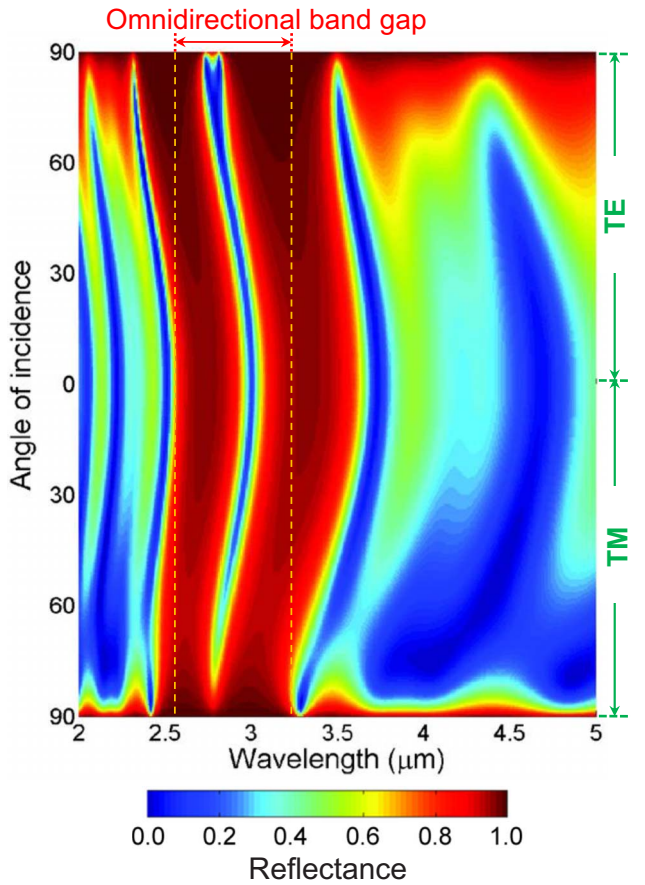

FIG. 4. (Color online) Calculated reflectance spectra of the omnidirectional filter as a function of wavelength for TM and TE polarizations for all angles of incidence at a position having the band gap centered around 3 μm.

The IR filter consists of alternating layers of low-index (As_2S_3) and high-index (GAST) glasses on a silicon substrate. In accordance with the simulation results, ten pairs of alternating As_2S_3 and GAST layers are thermally evaporated with thicknesses, 322 and 233 nm, respectively, to produce a photonic stop band centered at 3 μm [Fig. 1(c)]. The As_2S_3 cavity layer is located at the 13th layer from the top with a thickness of 644 nm. The graded thickness profile is obtained by simply giving a slant to the substrate with respect to the horizontal during thermal deposition [Fig. 1(a)]. In our case, a 40° slant gives a thickness profile for As_2S_3 (GAST) layer from 193 nm (140) to 365 nm (264) along the 5 cm substrate.

In order to determine the position dependence of the cavity mode, Fourier transform IR (FTIR) spectroscopy measurements in reflection mode are made along the substrate (Bruker FTIR Vertex 70 with Hyperion microscope). As shown in Fig. 3(a), the cavity mode shifts from 1.8 to 3.4 μm from one edge ($x=0$) of the substrate to the other ($x=5$ cm). Note that position dependence of the cavity mode is not exactly linear due to the thermal evaporation geometry. The calculated reflection spectrum for the filter position having the band gap centered around 3 μm agrees well with the measured results [Fig. 3(b)].

Furthermore, the reflectance spectra of the filter are investigated for oblique angles by performing simulations for the filter position having the cavity mode centered at 3 μm. Using the generalized transfer matrix method, the reflectance spectra are determined for all incidence angles and both TE/TM polarizations. Figure 4 shows the calculated reflec-

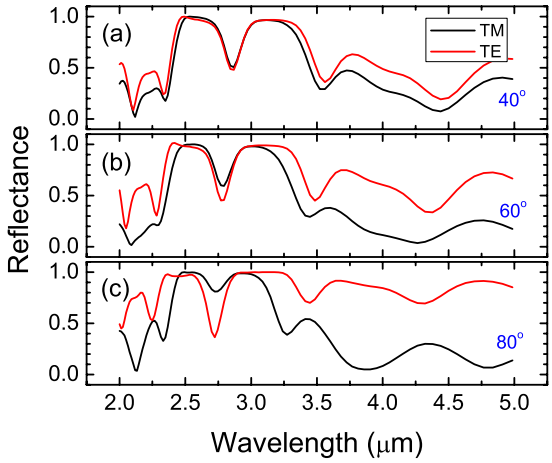

FIG. 5. (Color online) Measured reflectance spectra of the filter as a function of wavelength for (red lines) TE and (black lines) TM polarization modes at (a) 40°, (b) 60°, and (c) 80° angles of incidence.

tion spectra for incidence angles ranging from 0° to 90°. While the omnidirectional band gap extends from 2.6 to 3.3 μm, the cavity mode shifts to lower wavelengths as incidence angle increases. The omnidirectional reflections are also confirmed by the ellipsometric measurements at various incidence angles. Reflection spectra at three oblique angles are shown in Fig. 5 for all polarizations. The cavity mode is more sensitive to higher incidence angles to TM polarization.

The reflection spectra shown in Fig. 4 demonstrate that the peak wavelength of the cavity mode in the stop band is rather insensitive to angles of incidence. This makes the fabricated devices particularly suitable for IR spectral imaging and spectrometry. Using a hot filament as a source, even under poor collimation conditions, the filters effectively pass a narrow band of the IR radiation based on the spatial position. Applications of variable wavelength all-chalcogenide IR filters may potentially include portable (miniaturized) IR spectrometers, disposable chemical, and biological sensors. In addition, thermomechanical compatibility of such glasses enables thermal drawing of low-loss photonic band gap transmission[4] and externally reflecting fibers,[13] and on-fiber optoelectronic devices[5] at IR region. It is also possible to fabricate hollow-core omnidirectional on-chip waveguide structures for photonic applications at near- and mid-IR wavelengths.[20]

This work is supported by TUBITAK under the Contract Nos. 106T348, 106G090, and 107T547. M.B. acknowledges support from the Turkish Academy of Sciences Distinguished Young Scientist Award (TUBA GEBIP). This work was performed at the UNAM-Institute of Materials Science and Nanotechnology which is supported by State Planning Organization of Turkey through the National Nanotechnology Research Center Project.

[1] P. Yeh, A. Yariv, and C.-S. Hong, J. Opt. Soc. Am. **67**, 423 (1977).
[2] J. N. Winn, Y. Fink, S. Fan, and J. D. Joannopoulos, Opt. Lett. **23**, 1573 (1998).
[3] Y. Fink, J. N. Winn, S. H. Fan, C. P. Chen, J. Michel, J. D. Joannopoulos, and E. L. Thomas, Science **282**, 1679 (1998).
[4] B. Temelkuran, S. D. Hart, G. Benoit, J. D. Joannopoulos, and Y. Fink, Nature (London) **420**, 650 (2002).
[5] M. Bayindir, F. Sorin, A. F. Abouraddy, J. Viens, S. D. Hart, J. D. Joannopoulos, and Y. Fink, Nature (London) **431**, 826 (2004).
[6] A. F. Abouraddy, M. Bayindir, G. Benoit, S. D. Hart, K. Kuriki, N. Orf, O. Shapira, F. Sorin, B. Temelkuran, and Y. Fink, Nature Mater. **6**, 336 (2007).
[7] M. Bayindir, A. F. Abouraddy, O. Shapira, J. Viens, D. Saygin-Hinczewski, F. Sorin, J. Arnold, J. D. Joannopoulos, and Y. Fink IEEE J. Sel. Top. Quantum Electron. **12**, 1202 (2006).
[8] J. S. Sanghera, L. B. Shaw, and I. D. Aggarwal, C. R. Chim. **5**, 873 (2002).
[9] J.-F. Carlin, C. Zellweger, C. Dorsaz, S. Nicolay, G. Christmann, E. Feltin, R. Butte, and N. Grandjean, Phys. Status Solidi B **242**, 2326 (2005).
[10] R. M. Almeida, A. S. Rodrigues, J. Non-Cryst. Solids **326**, 405 (2003).
[11] E. W. Baumgartner, T. Schwarzl, G. Springholz, and W. Heiss, Appl. Phys. Lett. **89**, 051110 (2006).
[12] T. Kohoutek, J. Orava, T. Wagner, M. Hrdlicka, M. Vlcek, and M. Frumar, J. Phys. Chem. Solids **69**, 2070 (2008).
[13] S. D. Hart, G. R. Maskaly, B. Temelkuran, P. H. Prideaux, J. D. Joannopoulos, and Y. Fink, Science **296**, 510 (2002).
[14] A. Zakery and S. R. Elliott, J. Non-Cryst. Solids **330**, 1 (2003).
[15] B. Bureau, X. H. Zhang, F. Smektala, J.-L. Adam, J. Troles, H. Ma, C. Boussard-Pledal, J. Lucas, P. Lucas, D. L. Coq, M. R. Riley, and J. H. Simmons, J. Non-Cryst. Solids **345**, 276 (2004).
[16] C. C. Katsidis and D. I. Siapkas, Appl. Opt. **41**, 3978 (2002).
[17] M. Bayindir, A. F. Abouraddy, J. Arnold, J. D. Joannopoulos, and Y. Fink, Adv. Mater. (Weinheim, Ger.) **18**, 845 (2006).
[18] V. K. Tikhomirov, D. Furniss, A. B. Seddon, J. A. Savage, P. D. Mason, D. A. Orchard, and K. L. Lewis, Infrared Phys. Technol. **45**, 115 (2004).
[19] R. A. Synowicki and T. E. Tiwald, Thin Solid Films **455**, 248 (2004).
[20] Y. Yi, S. Akiyama, P. Bermel, X. Duan, and L. C. Kimerling, Opt. Express **12**, 4775 (2004).